G&G
Gem News International

Contributing Editors
Emmanuel Fritsch, *University of Nantes, CNRS, Team 6502, Institut des Matériaux Jean Rouxel (IMN), Nantes, France* (fritsch@cnrs imn.fr)
Gagan Choudhary, *Gem Testing Laboratory, Jaipur, India* (gagan@gjepcindia.com)
Christopher M. Breeding, *GIA, Carlsbad* (christopher.breeding@gia.edu)

COLORED STONES AND ORGANIC MATERIALS

Preliminary observations on facet-grade ruby from Longido, Tanzania. With rubies discovered about 100 years ago, the Longido district of Tanzania is one of the longest-known occurrences in Africa. The deposit is famous for its "ruby-in-zoisite," consisting of large red corundum crystals in a striking green zoisite matrix, often speckled with black amphibole spots. The majority is used for carving, but occasionally facet-quality material is discovered (D. Dirlam et al., "Gem wealth of Tanzania," Summer 1992 *G&G*, pp. 80–102).

For this study, 16 transparent rubies (figure 1) were collected during a July 2016 field expedition. The stones were acquired at the Mundarara mine in Longido and from a dealer in a nearby trading post. Most of the rough material ranged from 1 to 3 ct, although one heavily fractured piece weighed about 7 ct. Colors ranged from red to purplish red, very similar to the color of high-quality Mozambican ruby. Fluorescence was medium red under long-wave UV and weak red under short-wave UV.

Figure 1. Sixteen samples of facet-quality ruby (0.8–7.1 ct) from Longido, Tanzania. Photo by Sasithorn Engniwat.

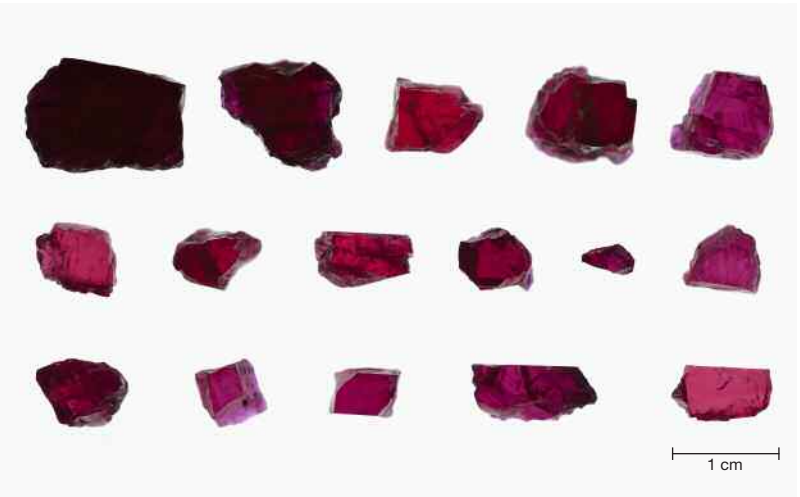

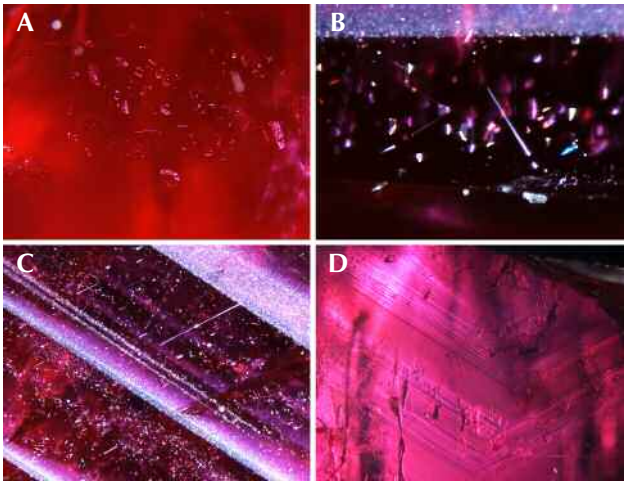

Figure 2. Internal features of ruby from Longido, Tanzania. A: A group of irregular thin films; field of view 1.6 mm. B: An array of reflective platelets with needles; field of view 0.9 mm. C: Short and long needles together with thin films; bands of fine reflective particles are also seen. Field of view 2.0 mm. D: Angular internal growth; field of view 4.0 mm. Photomicrographs by Boodsakorn Kongsomart.

The inclusion scenes (figure 2) had features similar to those of rubies from Mozambique: short needles, particle

Editors' note: Interested contributors should send information and illustrations to Stuart Overlin at soverlin@gia.edu or GIA, The Robert Mouawad Campus, 5345 Armada Drive, Carlsbad, CA 92008.

Gems & Gemology, Vol. 53, No. 4, pp. 472–490.

TABLE 1. Trace element concentrations in rubies from East African deposits.

Source		Trace element (ppma)				
Country	Mine	Cr min-max (avg., SD)	Fe min-max (avg., SD)	Ga min-max (avg., SD)	Mg min-max (avg., SD)	V min-max (avg., SD)
Tanzania	Longido, facet-grade (n=16)	1604–5059 (3300, 791)	62–544 (403, 80)	6–10 (7, 1)	7–42 (13, 7)	3–25 (5, 4)
	Longido, carving-grade (n=5)	1839–6235 (3760, 1185)	350–868 (565, 151)	5–8 (6, 0)	9–130 (32, 31)	2–4 (3, 0)
	Winza, facet-grade (n=14)	161–1094 (583, 295)	405–1596 (816, 276)	4–11 (6, 1)	0–118 (22, 21)	0–1 (1, 0)
Mozambique	Montepuez, Mugloto, facet-grade (n=14)	506–1737 (1167, 318)	851–2034 (1534, 243)	5–12 (9, 1)	11–50 (24, 10)	2–7 (4, 1)
	Montepuez, Maninge Nice, facet-grade (n=5)	1886–4941 (2868, 813)	261–402 (331, 30)	6–9 (7, 1)	19–47 (31, 8)	1–6 (3, 1)
Madagascar	Didy, facet-grade (n=21)	33–2698 (440, 498)	533–1274 (856, 198)	3–17 (8, 4)	0–67 (13, 14)	2–17 (5, 4)
	Andilamena, facet-grade (n=14)	53–1569 (403, 377)	559–1559 (1009, 253)	7–21 (14, 4)	19–53 (36, 7)	4–29 (18, 7)
	Zahamena, facet-grade (n=66)	135–3922 (1196, 874)	284–1994 (912, 249)	10–30 (16, 4)	13–61 (35, 8)	10–100 (17, 11)
Malawi	Chimwadzulu, facet-grade (n=18)	269–1816 (648, 377)	953–2760 (1697, 497)	5–15 (8, 3)	10–39 (21, 6)	1–10 (5, 2)

n = number of samples analyzed. On each sample, a minimum of three spots were measured. All the samples were facet grade except those from Longido, Tanzania, which included both facet and carving grades.

banding, and reflective platelets (V. Pardieu et al., "Rubies from the Montepuez area, Mozambique," *GIA News from Research*, Oct. 1, 2013). The most common inclusions were thin films (figure 2A), a combination of needles and reflective platelets (figure 2B), and particle banding (figure 2C). In addition, dense particulate planar clouds were arranged mostly parallel to each other and associated with short and long needles (again, see figure 2C). Internal growth zones (figure 2D) and twinning features were also found. Several types of crystals were identified by Raman spectroscopy, including amphibole, mica, and feldspar. Undetermined opaque metallic inclusions were also observed.

Various advanced analytical techniques were used to characterize the properties of the studied rubies. Fourier-transform infrared (FTIR) spectroscopy revealed strong absorption features consistent with boehmite in all samples. Other minerals that are normally present in ruby, such as diaspore or kaolinite, were not detected in the studied rubies.

The trace element concentrations of these rubies were analyzed with laser ablation–inductively coupled plasma–mass spectrometry (LA-ICP-MS) and compared to ruby from other East African sources (table 1). The rubies from Longido were extremely rich in Cr and fairly low in Fe compared to other African sources. The only East African deposit producing ruby with similar concentrations of chromophores is Maninge Nice in Mozambique, but the facet-grade material from Longido has lower magnesium content on average. Other deposits can be separated from Longido based on other trace elements (again, see table 1), although minor overlap cannot be excluded.

While Longido is traditionally known for large ruby-in-zoisite specimens, facet-grade rough is also produced and can yield attractive gemstones. Chemical analysis revealed an extremely high chromium concentration in both facet- and carving-grade ruby. While the internal features of the rubies from Longido are quite similar to those of other African deposits, trace element composition can aid in positively identifying their origin.

Boodsakorn Kongsomart, Wim Vertriest, and Vararut Weeramonkhonlert
GIA, Bangkok

Figure 3. A selection from Campbell Bridges's tsavorite collection, displayed at the 2017 AGTA Tucson Gem Fair. This collection includes some of the most important pieces found in the past half century. Photo by Robert Weldon/GIA, courtesy of the Bridges family.

Celebrating 50 years of tsavorite. The year 2017 marked the 50th anniversary of Campbell Bridges's discovery of tsavorite. At the 2017 AGTA Tucson Gem Fair, the Smithsonian Institution hosted a selection of historical pieces from Bridges's personal collection to commemorate his life's work (figure 3).

Starting in the front row and proceeding from left to right, we begin with two crystals that are some of the first tsavorites Bridges discovered, near Komolo, Tanzania, in 1967. These are among the first samples that were analyzed to identify this new gemstone.

Next, the tsavorite in matrix represents the 1970 discovery in Taita, Kenya, at Bridges's GG3 mine. Also represented from this location is a lovely tsavorite "thumbnail" unearthed in 1971. Some years prior, Bridges was engaged by Tiffany & Co. as a consultant. He was the first to bring tanzanite to the United States, and was credited with the discovery of tsavorite in Tiffany ads introducing the gem to the public in 1974 (figure 4).

The three large tsavorite rough samples weighing more than 5 grams each were found in 1980 at a source Bridges christened the Scorpion mine. The vibrant yet rich pure green to bluish green hue became a well-known characteristic of material from this mine. Over the following four decades, the Scorpion mine would prove to be the world's most prolific producer of fine tsavorite.

The next six rough pieces, weighing 5 to 25 grams, were recovered in 1992 from the famed Bonanza tunnel at the Scorpion mine. The Bonanza tunnel is the richest tsavorite-bearing reef zone at Scorpion and has yielded some of the finest pockets the world has seen. The "saddle reef structure," a series of recumbent folds, is the characteristic geological feature identified by Bridges at the Scorpion mine. This distinctive structure has led to the mine's rich and consistent production throughout its history.

Rounding out the Scorpion mine material in the top left corner is an extremely rare terminated euhedral tsavorite crystal in matrix. As tsavorite occurs under very high pressures and temperatures, it is often highly fractured in rough form, making such an unblemished and well-formed specimen a remarkable occurrence.

Figure 4. In this 1973 photo, Campbell Bridges (right) discusses tsavorite with Henry B. Platt, former president of Tiffany & Co. Photo courtesy of the Bridges family.

In the top right corner, we have a tsavorite nodule in matrix that opens a window into the gem's formation and its associated minerals. This nodule was extracted in its entirety from the Bonanza reef three decades ago and kept intact.

On display (again, see figure 3) are tsavorite, surrounded in the matrix by tanzanite, calcite, pyrite, quartz, and graphite. Tsavorite and tanzanite can occasionally occur together, though their formation is separated by approximately 100 million years. Tsavorite forms under prograde metamorphism and tanzanite under retrograde metamorphism.

Keeping guard on this tsavorite bounty are the namesakes of the Scorpion mine. These pewter scorpions were directly cast from actual scorpions that patrolled the mine. Needless to say, it's advisable to check your shoes in the morning… Also on display is one of Campbell Bridges's earliest business cards, from 1967.

In the top row are four extraordinarily fine, loupe-clean faceted gemstones. None of these were ever on public display before the Tucson exhibit. The first is a lovely 25.10 ct "mint" green grossular garnet, unearthed in 1971 from Bridges's GG2 mine in Taita, Kenya. Interestingly, this color of mint green garnet has been found at all of the Bridges mines in Tanzania and Kenya over the decades. A strike may yield both richly colored high-chromium and vanadium-colored saturated tsavorite, as well as the far lighter, mint green garnet within the same pocket. This variety is most prevalent in Merelani, Tanzania, but also occurs near Komolo, Tanzania, as well as in Taita. While such material came from all three locations in the early years, it simply was not marketable back then. It was not until the 2000s that a real market for these garnets developed.

Next is an exceptional 31.27 ct oval from Merelani with a vivid blue-green color. This tsavorite retains fantastic brilliance even in low lighting, while maintaining a sufficient level of saturation under strong lighting.

Last but certainly not least are two tsavorite cushions. As to their origin, the Bridges family wishes to preserve an element of mystery. The 33.55 ct square cushion on the right is a loupe-clean gem exhibiting an exceptional blue-green color that is well saturated yet extraordinarily vivid. After a lifetime of dealing with tsavorite, the author considers this one of the finest examples ever produced between 10 and 50 carats.

The largest of the four faceted gemstones in this display is a 58.52 ct cushion. It is another loupe-clean example representing the pinnacle of what is possible in tsavorite. It also exhibits a strong blue-green color that glows in any lighting environment. This is the finest tsavorite above 50 ct observed by this author. Given its one-of-a-kind nature, the Bridges family felt it most appropriate to name the gem the "Golden Jubilee" in honor of tsavorite's 50th anniversary.

As tsavorite and the legacy of Campbell Bridges celebrate 50 years, the Bridges family wishes to thank the Smithsonian and the colored gemstone community for their support throughout the years.

Bruce Bridges
Bridges Tsavorite, Nairobi

New azurite-malachite mixture from Peru. Green malachite, $Cu_2(CO_3)(OH)_2$, is very popular as an ornamental stone, with huge quantities coming every year from deposits in the Katanga Province of the Democratic Republic of Congo. Blue azurite has a similar chemical composi-

Figure 5. This polished vein of azurite with malachite and chrysocolla mined from Cochapata measures 8.5 cm wide. Photo by J. Hyršl.

Figure 7. A cross-section of a 25-mm-wide malachite double stalactite from Cochapata. The stalactite on the right shows malachite with an azurite center. Photo by J. Hyršl.

tion, $Cu_3(CO_2)_2(OH)_2$, but is much more rare. Cabochons of pure azurite are usually quite dark and not very attractive. A blend of the two is much more appealing for jewelry, but this combination is seldom found. Attractive azurite-malachite mixtures are known mainly from old finds in Bisbee and Morenci, both in the U.S. state of Arizona. There was also a find of malachite-azurite-gypsum mixture from Peru's Moquegua region in 2012 (J. Hyršl, "Malachite-azurite from Peru," *Journal of Gemmology*, Vol. 34, No. 7, 2015, p. 564).

Another new azurite-malachite mixture appeared in 2016 and was originally described as from Puno, in southeastern Peru. In fact, it is from Cochapata, in the Cotabambas Province about 50 km southwest of Cuzco, situated in high mountains. According to a dealer who visited the locality, there are several outcrops of oxidized copper veins on a steep hill exploited by artisanal miners. The veins are up to about 20 cm wide, but the parts most useful for cutting are usually only a few centimeters wide. Several tons of the rough have already been sold in Lima to foreign dealers, with the largest piece weighing 80 kg.

Deep blue azurite is the main mineral found today in Cochapata, accompanied by light green malachite and, less commonly, light blue chrysocolla (figure 5). The most attractive specimens have malachite with a banded structure, but some possess a brecciated structure (figure 6). The rarest samples are stalactites of malachite up to 5 cm in length. Some were sliced perpendicular to the elongated growth direction to prepare very attractive stones with an agate-like structure (figure 7).

Jaroslav Hyršl (hyrsl@hotmail.com)
Prague

Figure 6. These azurite-malachite cabochons, fashioned from Cochapata material, measure up to 31 mm. Photo by J. Hyršl.

DIAMONDS

Two natural type IIa diamonds with strong phosphorescence and Ni-related defects. Strong phosphorescence under UV excitation is rarely seen in natural diamond and normally limited to hydrogen-rich type Ia or type IaA/Ib chameleons and type IIb diamonds (T. Hainschwang et al., "A gemological study of a collection of chameleon diamonds," Spring 2005 *G&G*, pp. 20–35; S. Eaton-Magaña and R. Lu, "Phosphorescence in type IIb diamonds," *Diamond and Related Materials*, Vol. 20, No. 7, 2011, pp. 983–989). When seen in other diamond types, an even rarer occurrence, it is shorter and less intense. Recently, the National Gemstone Testing Center (NGTC) in Beijing encountered two natural diamonds that showed extraordinarily strong blue phosphorescence and uncommon fluorescence colors under the DiamondView.

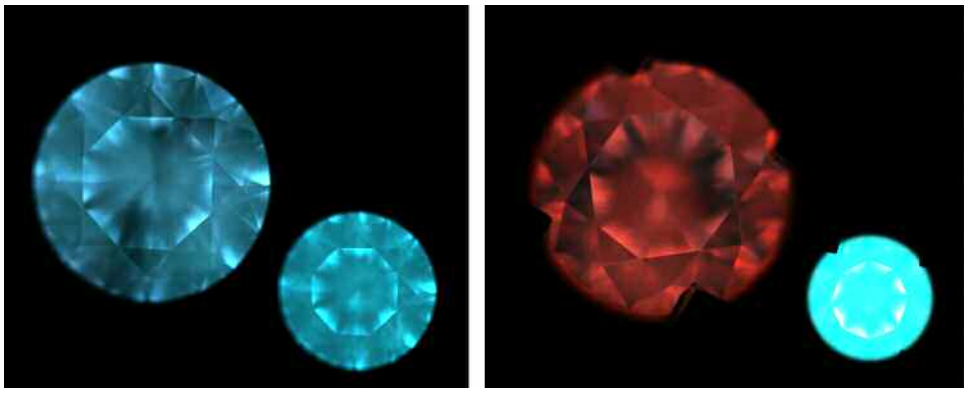

Figure 8. DiamondView images of two unusual diamonds (0.18 and 0.30 ct, respectively). Left: Unevenly distributed grayish blue fluorescence and strong blue phosphorescence. Right: Vivid red fluorescence, strong blue phosphorescence, and a dislocation network can be seen in the table. Images by Shi Tang.

The diamonds weighed 0.18 and 0.30 ct and were both graded as E color. Both were type IIa, with neither nitrogen absorption between 1100 and 1400 cm^{-1} nor boron-related absorption in their infrared spectra. Magnification and examination with a standard UV lamp showed no abnormal phenomena for natural type IIa diamonds. Instead of the deep blue fluorescence and inert phosphorescence that natural type IIa diamonds typically show in DiamondView imaging, the 0.18 ct diamond emitted unevenly distributed grayish blue fluorescence and strong blue phosphorescence, similar to that of a colorless HPHT synthetic diamond. The 0.30 ct diamond displayed vivid red fluorescence and strong blue phosphorescence, which is unusual for a natural colorless to near-colorless diamond (figure 8). Red fluorescence is rare in natural type IIa diamond and seldom reported (Summer 2016 Lab Notes, pp. 189–190).

Photoluminescence (PL) spectra collected with 532 nm laser excitation at liquid nitrogen temperature revealed something even more interesting. Along with the GR1 center emission at 741 nm typically seen in natural type IIa diamonds, the 883.0/884.7 nm doublet that is related to nickel impurity appeared in both samples' PL spectra (figure 9). This doublet, often referred to as the "1.40 eV center," is frequently seen in the {111} growth sectors of HPHT synthetic diamonds produced using Ni-based solvents/catalysts. Ni-related defects are more often seen in natural chameleon and greenish yellow diamonds (W. Wang et al., "Natural type Ia diamond with green-yellow color due to Ni-related defects," Fall 2007 *G&G*, pp. 240–243; Summer 2014 Lab Notes, pp. 151–152) but seldom found in colorless to near-colorless natural diamonds (e.g., Spring 2017 Lab Notes, pp. 95–96). For natural diamonds

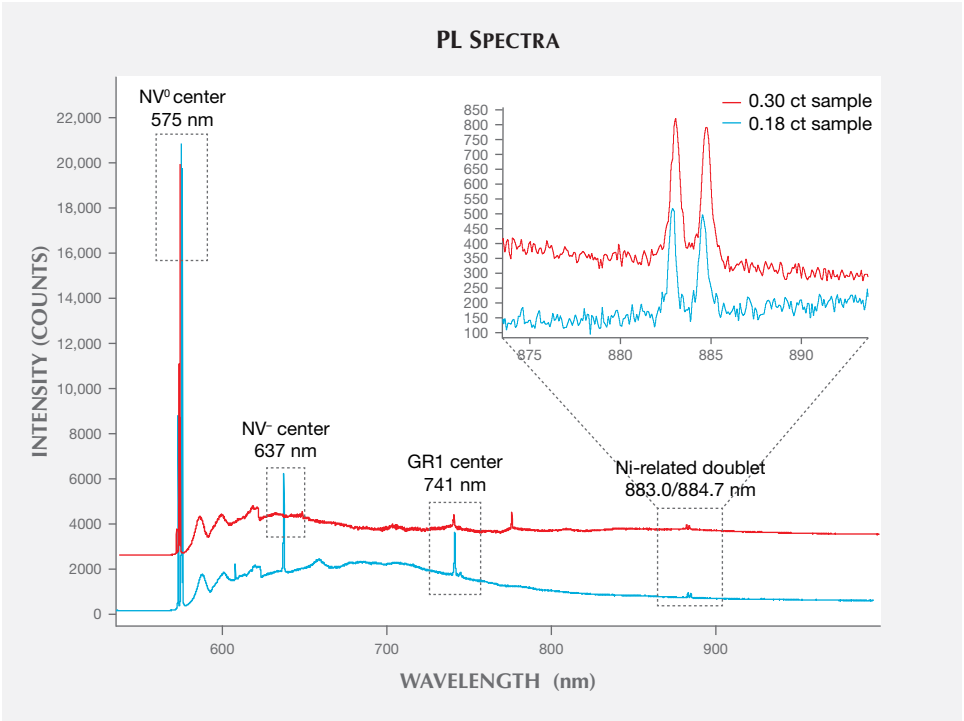

Figure 9. PL spectra of the two samples with 532 nm laser excitation. Both showed weak Ni-related doublets at 883.0/884.7 nm and strong NV centers at 575 and 637 nm, as well as the GR1 center at 741 nm.

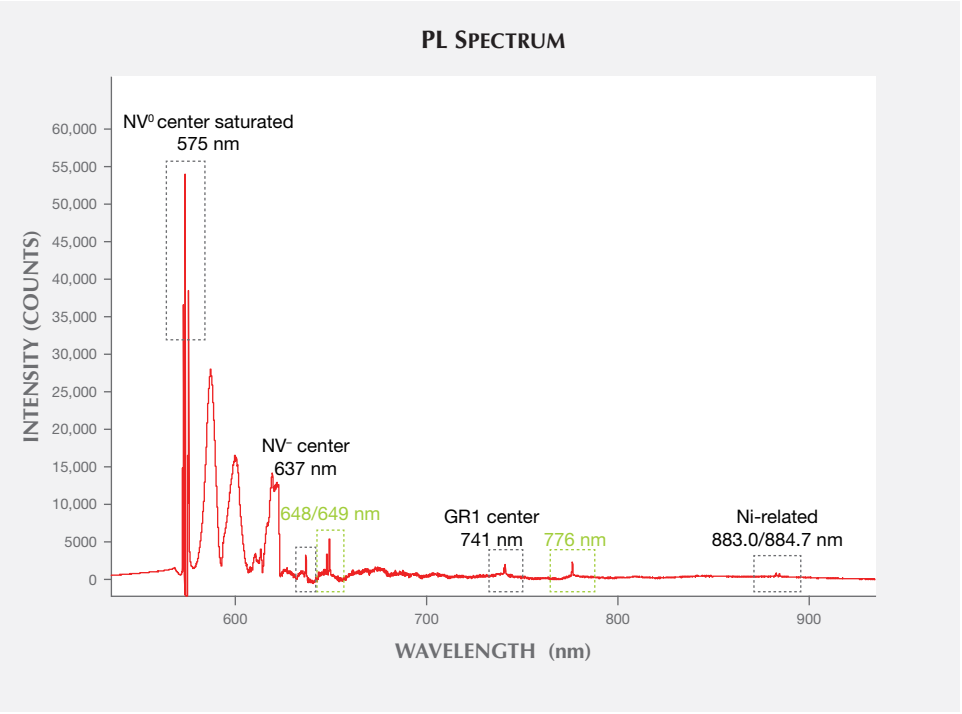

Figure 10. The PL spectrum of the 0.30 ct sample emitted with a 532 nm laser, at higher excitation energy. The NV^0 center peak is saturated, and emissions at 648 and 776 nm are clearly seen.

with such strong phosphorescence, the presence of Ni-related emissions is unusual.

The PL spectrum of the 0.30 ct sample also presented an extremely strong NV center at 575 nm, compared to the diamond emission at 572 nm, which explained the reddish fluorescence in the DiamondView image. In each sample's PL spectrum, the relative intensity of NV^0 (575 nm) is significantly stronger than that of NV^- (637 nm).

Furthermore, when we exposed the 0.30 ct sample to higher-energy excitation with the 532 nm laser to reveal more subtle features, the PL spectrum showed moderately strong emissions at 648/649 nm and 776 nm (figure 10). According to previous research, PL peaks at 648.2 and 776.4 nm are associated with boron in phosphorescing type IIb natural diamonds (Eaton-Magaña and Lu, 2011). Later studies ascribed the 648.2 nm defect to a boron-interstitial complex, while the 776.4 nm peak was assigned to a B-V complex (S. Eaton-Magaña and T. Ardon, "Temperature effects on luminescence centers in natural type IIb diamonds," *Diamond and Related Materials*, Vol. 69, 2016, pp. 86–95). These emissions may partly explain the strong phosphorescence of the 0.30 ct sample. Since they were not detected in the 0.18 ct sample, which also exhibited strong phosphorescence—the same is true of other phosphorescent natural IIa diamonds the authors have encountered before—this cannot be the full explanation.

Despite the synthetic-like luminescence color in DiamondView imaging and the Ni-related emissions in the PL spectra, the samples' Fourier-transform infrared (FTIR) spectra, UV-visible spectra, PL spectra, features observed under the crossed polarizing microscope, and UV reaction indicated that they are not of synthetic origin. These two samples demonstrated the diversity of luminescence and spectral features found in natural diamond. Their identification also highlights the importance of a comprehensive understanding of diamond origin.

Shi Tang (tangs@ngtc.com.cn), Zhonghua Song, Taijin Lu, Jun Su, and Yongwang Ma
NGTC, Beijing

Interesting growth structure in black diamond. The color of most black diamonds is attributed to graphite micro-inclusions or metallic inclusions (S.V. Titkov et al., "An

Figure 11. This 1.03 ct opaque round brilliant cut with a striking pattern of micro-inclusions was identified as a black diamond. Photo by Yujie Li.

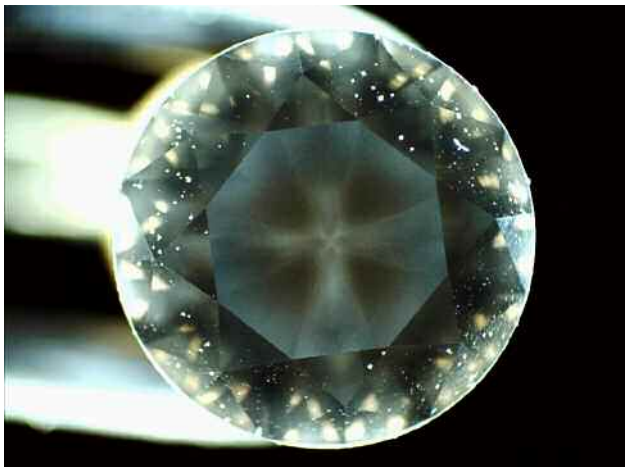

Figure 12. The "double cross" pattern seen in the black diamond. This pattern showed that the small inclusions were restricted to certain sectors, indicating that the diamond crystallized through two separate processes. Photo by Yujie Li; field of view approximately 4 mm.

investigation into the cause of color in natural black diamonds from Siberia," Fall 2003 *G&G*, pp. 200–209), and it is rare to see dense clouds of micro-inclusions producing a black appearance (see Spring 2007 Lab Notes, pp. 52–53). Since November 2016, the National Gemstone Testing Center (NGTC) in Shanghai has routinely received large quantities of polished black diamonds. One such stone, a 1.03 ct opaque round brilliant (figure 11) that we believed to have been heat treated, had a striking pattern of microinclusions we had never seen before.

Figure 13. The pattern as seen in the DiamondView. The well-developed cuboid growth sectors exhibited yellowish green fluorescence, while the poorly developed octahedral growth sectors were inert to the short-wave UV light. The DiamondView also revealed a mixed-habit growth structure.

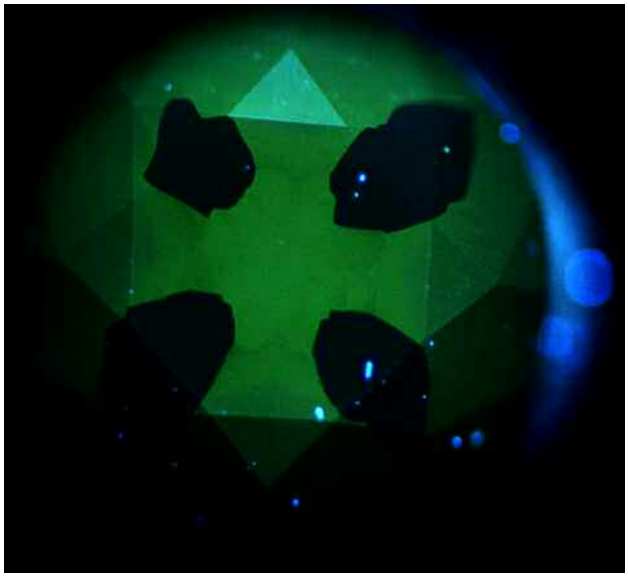

Microscopic observation revealed a "double cross" pattern arising from an abundance of pinpoint-like gray inclusions restricted to certain sectors of the diamond (figure 12). The outer black cross was oriented in the same direction as the inner pale cross. The inclusions' crystalline forms were too small to resolve at 40× magnification. These small inclusions absorbed a large proportion of the light entering the diamond, causing the black appearance. The FTIR absorption spectrum confirmed the diamond was type IaAB and H-rich, with nitrogen-related absorption from 1000 to 1500 cm^{-1}, a graphite-related peak at 1582 cm^{-1}, and H-related IR peaks at 1405, 2785, 3050, 3107, 3154, 3236, 4169, and 4496 cm^{-1}. We confirmed that the pinpoint-like inclusions were graphitized hydrogen clouds (see P. Johnson et al., "Hydrogen rich treated black diamonds," poster presentation at Geological Society of America 2016 annual meeting).

When observed in the high-energy short-wave UV radiation of the DiamondView (figure 13), the bulk of this black diamond displayed moderate yellowish green fluorescence. Four small areas were basically inert to UV radiation; these also corresponded to the dark cross.

The unique double cross pattern and the DiamondView image revealed an interesting growth structure. The diamond apparently underwent two distinct phases of growth, with each phase forming a cross developing from separate mixed-habit growth with contemporaneous cuboid and octahedral sectors. The well-developed cuboid growth sectors contained regions with cloud-like light scattering that caused the black parts; very poorly developed octahedral growth sectors with a small amount of inclusions formed the light cross. The cuboid growth sectors exhibited yellowish green fluorescence, while the inclusion-poor octahedral sectors were inert to the short-wave UV light.

The interesting pattern of inclusions and distinctive growth features of black diamonds such as this one needs more attention.

Contributors' note: This study was supported in part by the National Natural Science Foundation of China (grants 41473030 and 41272086).

Yujie Li, Hui Xu, Taijin Lu, Zhikun Hu, and Xinming Wang
NGTC, Shanghai

The Foxfire diamond, revisited. The largest gem-quality rough diamond found in Canada, reported earlier in *Gems & Gemology* (Summer 2016 GNI, pp. 188–189), has revealed remarkable responses to excitation with long- and mid-wave UV light. This 187.63 ct diamond (figure 14) was extracted from the Diavik mine in the Canadian Arc-

Figure 14. The 187.63 ct Foxfire rough diamond. Photo by Jeffrey Post.

tic in the spring of 2015. Aptly named for the aurora borealis, the "Foxfire" displays unusual fluorescence and phosphorescence behavior upon exposure to ultraviolet light. As previously reported, this type Ia diamond has a high concentration of nitrogen impurities, a weak hydrogen-related absorption at 3107 cm^{-1}, and typical "cape" absorption lines.

Exposing this stone to the near-band-gap ultraviolet light of the DiamondView instrument (about 210 nm) and short-wave UV (253.7 nm) results in only very weak fluorescence and phosphorescence, as reported earlier. However, exposure to mid- and long-wave UV (313 nm and 365.0 nm, respectively) produces extremely strong blue fluorescence and strong, long-lived orangish phosphorescence (figure 15).

Another surprising result of exposing the Foxfire diamond to UV light is a noticeable color change from very pale yellow to a light brown color (figure 16). Fortunately, the diamond reverts to its original color in a matter of minutes in ambient room lighting.

We further examined the spectral characteristics of the UV-excited phosphorescence emission with the spectrometer previously used to study phosphorescence from the Hope and other colored diamonds (S. Eaton-Magaña et al., "Fluorescence spectra of colored diamonds using a rapid, mobile spectrometer," Winter 2007 *G&G*, pp. 332–351; S. Eaton-Magaña et al., "Using phosphorescence as a fingerprint for the Hope and other blue diamonds," *Geology*, Vol. 36, No. 1, 2008, pp. 83–86). In the present experiments, the UV light sources employed were mineralogical short-, mid-, and long-wave UV lamps. Figure 17 displays the spectral emission between 350 and 1000 nm (approximately 10 nm resolution) as a function of time after turning off the UV light. The most intense emission resulted from long- and mid-wave UV excitation, while phosphorescence excited by short-wave UV was extremely weak.

The spectra of the "orange" phosphorescence reported above are unusual and distinct from those of other natural and lab-grown phosphorescent diamonds we have examined. We speculate that the primary mechanism for phosphorescence in diamonds is light emission resulting from recombination of electrons trapped at ionized donors and holes trapped at ionized acceptors that are in close proximity to one another. The long time delay results from the thermal movement of the trapped electrons or holes to retrap close enough to one another (P.J. Dean et al., "Intrinsic and extrinsic recombination radiation from natural and synthetic aluminum-doped diamond," *Physical Review*, Vol. 140, No. 1A, 1965, p. A352–A386; B. Dischler et al., "Diamond luminescence: Resolved donor-acceptor pair recombination lines," *Diamond and Related Materials*, Vol. 3, 1994, pp. 825–830). In the case of the Foxfire, we cannot identify as yet the nature of either the acceptors or donors involved.

Similarly, the phenomenon of the observed color change from light yellow to light brown with UV excitation and the

Figure 15. Left: The Foxfire diamond, photographed in daylight-equivalent lighting. Center: The fluorescence exhibited in a darkened room while the diamond was exposed to long-wave UV. Right: The phosphorescence shown in a darkened room immediately after extinguishing long-wave UV excitation. Photos by Jeffrey Post.

Figure 16. The Foxfire under ambient room lighting, before (left) and just after exposure to long-wave UV light (right). Photos by Jeffrey Post.

reversal to light yellow has no detailed explanation yet. Such color changes, or sometimes a lightening of color, are often observed in natural diamonds. It is speculated that these are due to charge transfer between various defects (donor or acceptor states) within diamond. Diamond is inherently an insulator where electric charges move very slowly and their motion depends on the nature of the defects present, the temperature of the diamond, and its exposure to light. For an interesting discussion, see K.S. Byrne et al., "Chameleon diamonds: Thermal processes governing luminescence and a model for the color change," *Diamond and Related Materials*, Vol. 81, 2018, pp. 45–53.

James E. Butler and Jeffrey E. Post
Smithsonian Institution,
National Museum of Natural History
Washington, DC

Wuyi Wang
GIA, New York

TREATMENTS

Coated beryl imitating emerald. Two major issues related to emerald are origin determination and the presence and quantity of fillers. An emerald's value depends in part on the quality of the stone and treatments applied, so examination with a gemological microscope is an essential part of any analysis.

A pair of earrings (figure 18, top) weighing a total of 84.06 grams was submitted to the Lai Tai-An Gem Lab for identification. The earrings consisted of numerous green drilled briolettes with a vitreous luster. The client, who claimed they were natural emeralds, granted permission to remove one piece to aid in identification. Testing gave a spot RI of 1.57, an SG of 2.67, and an inert reaction to both short-wave and long-wave UV, consistent with beryl. Microscopic observation revealed liquid, crystal, and two-phase inclusions (figure 18, bottom). Infrared and Raman spectroscopy indicated that the loose stone, along with the similar stones still in the earrings, were beryl. Epoxy peaks at 3056, 3037, 2964, 2931, and 2872 cm^{-1} were obtained by FTIR spectroscopy (figure 19). However, the green color was unusual in that it appeared to be concentrated on the surface, which was confirmed by additional testing.

Magnification with diffused illumination clearly showed concentrated patches of green color with "colorless" boundaries (figure 20, left), as often seen in diffusion-

Figure 17. Phosphorescence emission vs. time after extinguishing long-wave (left), mid-wave (center), and short-wave UV excitation (right).

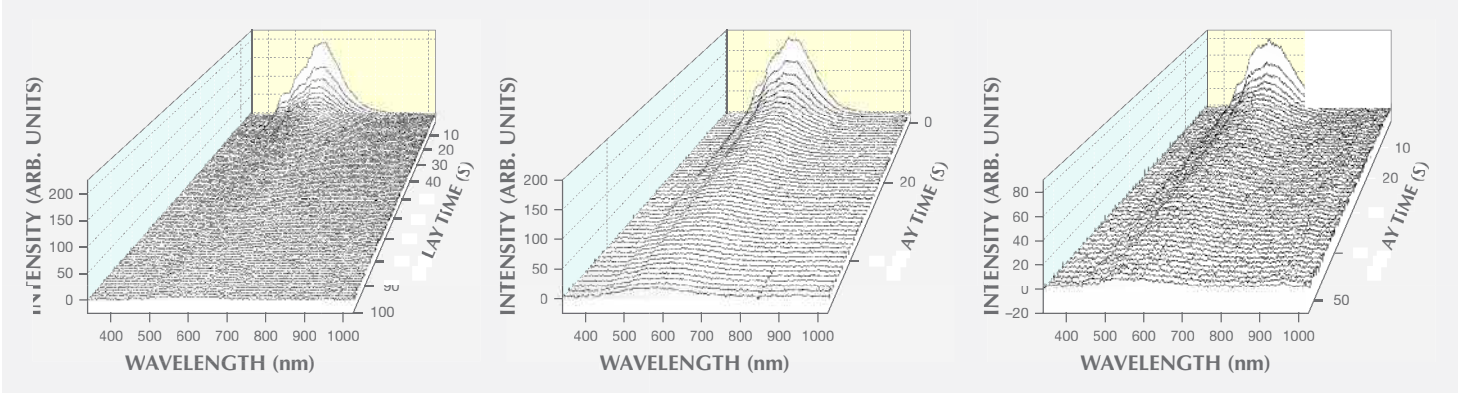

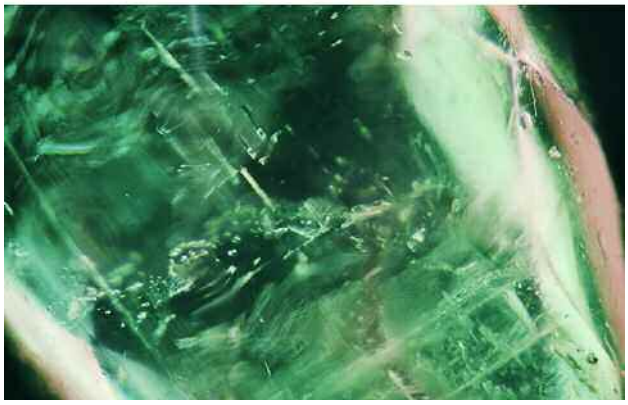

Figure 18. Top: The drilled green briolettes mounted in the pair of earrings submitted for identification. Bottom: Fluid inclusions, crystals, and two-phase inclusions proved the stones' natural origin; field of view 2.6 mm. Photos by Lai Tai-An Gem Lab.

treated stones such as corundum. Further observation by scanning electron microscopy (SEM) indicated a coating on the faceted surface (figure 20, right). DiamondView imaging revealed the fluorescence reaction of the underlying

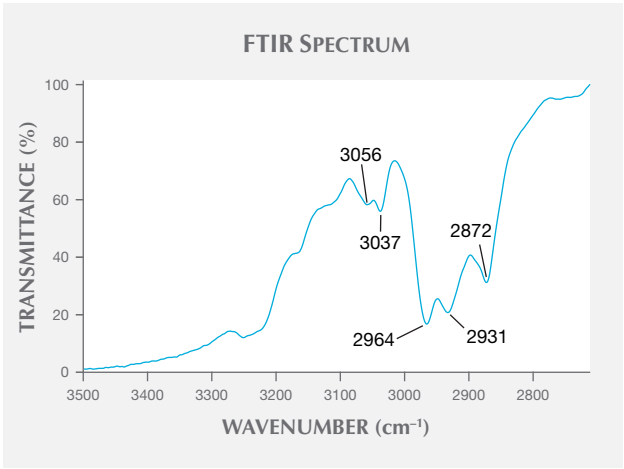

Figure 19. FTIR spectroscopy showed epoxy peaks at 3056, 3037, 2964, 2931, and 2872 cm^{-1}.

host beryl where the coating had been worn away at the facet junctions: When exposed to the ultra-short-wave UV of the DiamondView, the "colorless" areas reacted with a strong orange fluorescence (figure 21). UV-Vis-NIR spectra revealed differences between the test stone and a reference emerald. While emerald normally exhibits Cr^{3+}-associated main absorption bands at approximately 620 and 430 nm, the examined samples showed strong absorption bands at approximately 680 and 360 nm, as well as weaker bands at 620 and 430 nm (figure 22)

Coatings have been applied to various gemstones for decades, and most of the time they are easy to identify. Although this identification was not particularly challenging, it does show the importance of thoroughly examining jewelry in case treated stones have been incorporated into the design.

Larry Tai-An Lai (service@laitaian.com.tw)
Lai Tai-An Gem Laboratory, Taipei

Filled pearl with surface features. Pearl cultivation has been carried out for more than a century, with newer tech-

Figure 20. Left: Magnification with diffused illumination clearly showed the concentrated green areas of the coating and the boundaries of the underlying host beryl. Photomicrograph by Lai Tai-An Gem Lab; field of view 4.4 mm. Right: An SEM image from the specimen. The area labeled A shows the coated layer on the surface, while B shows facet boundaries without coating.

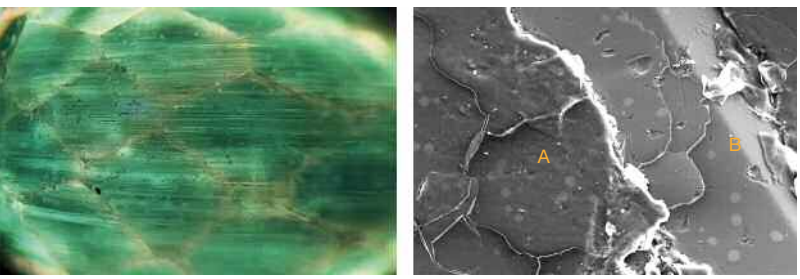

Figure 21. DiamondView imaging showed where the coating had been worn away at the facet junctions. The colorless areas reacted with a strong orange fluorescence after exposure to the short-wave UV radiation.

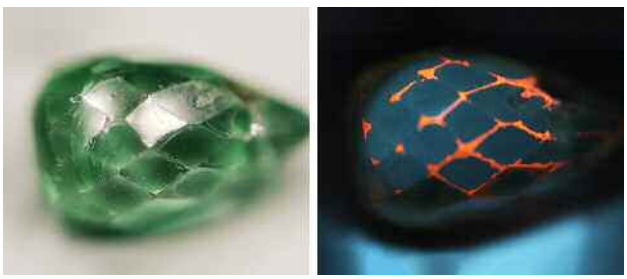

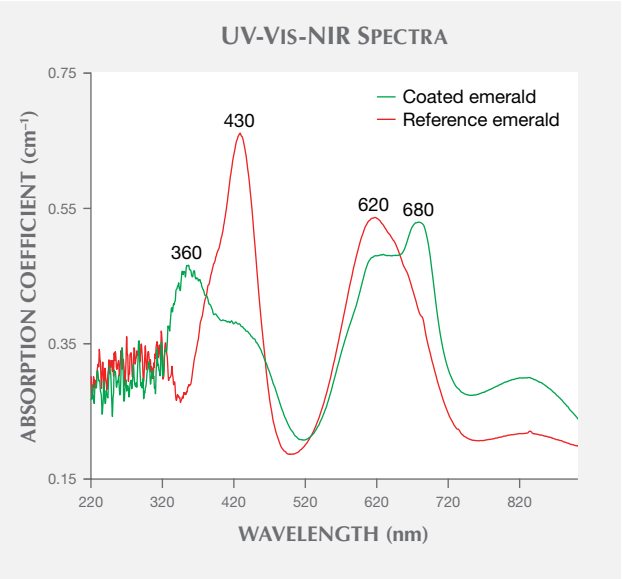

Figure 22. UV-Vis-NIR spectra show the differences between a reference emerald, which exhibits significant Cr^{3+}-associated main absorption bands at approximately 620 and 430 nm only (red trace), and the examined sample, which contains absorption bands at approximately 680 and 360 nm in addition to the 620 and 430 nm bands (green trace).

niques supplying the trade with larger and more consistently round freshwater and saltwater pearls. While natural pearls are seldom perfectly round, their rarity makes them desirable nevertheless. The Lai Tai-An Gem Lab recently had the chance to examine a specimen that was purchased by the client as a "natural white pearl" (figure 23) while traveling in the Philippines.

Figure 23. This 20.60 ct specimen was purchased by the client as a "natural white pearl." Photo by Lai Tai-An Gem Lab.

Figure 24. Two fillings displayed a coarse appearance and lower luster that differed from the rest of the pearl. Photomicrographs by Lai Tai-An Gem Lab; fields of view 11.5 mm (left) and 8.6 mm (right).

The white baroque pearl measured 20.0 × 19.0 × 13.3 mm and weighed 20.60 ct, with an SG of 2.60. It exhibited pink overtone. Long-wave UV produced a strong chalky blue reaction. Magnification revealed the typical overlapping platelet structure expected for nacreous pearls, but two abnormal surface features were also observed. These two areas displayed a coarse appearance and lower luster that differed from the rest of the pearl (figure 24).

We further analyzed the abnormal surface features to gather more data for future reference. DiamondView imaging showed a noticeable difference between the nacreous areas and the filled portions (figure 25). Raman analysis of the surface features revealed epoxy peaks at 635, 1108, and 1604 cm^{-1} and aragonite peaks at 1084 and 701 cm^{-1} (figure

Figure 25. The two filled portions of the pearl, shown in visible light (left images) and the DiamondView (right images). The DiamondView reaction showed a noticeable difference between the nacreous areas and the filled portions of the pearl.

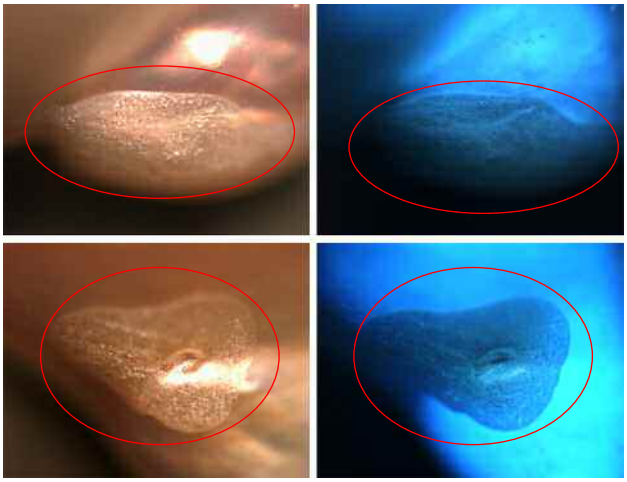

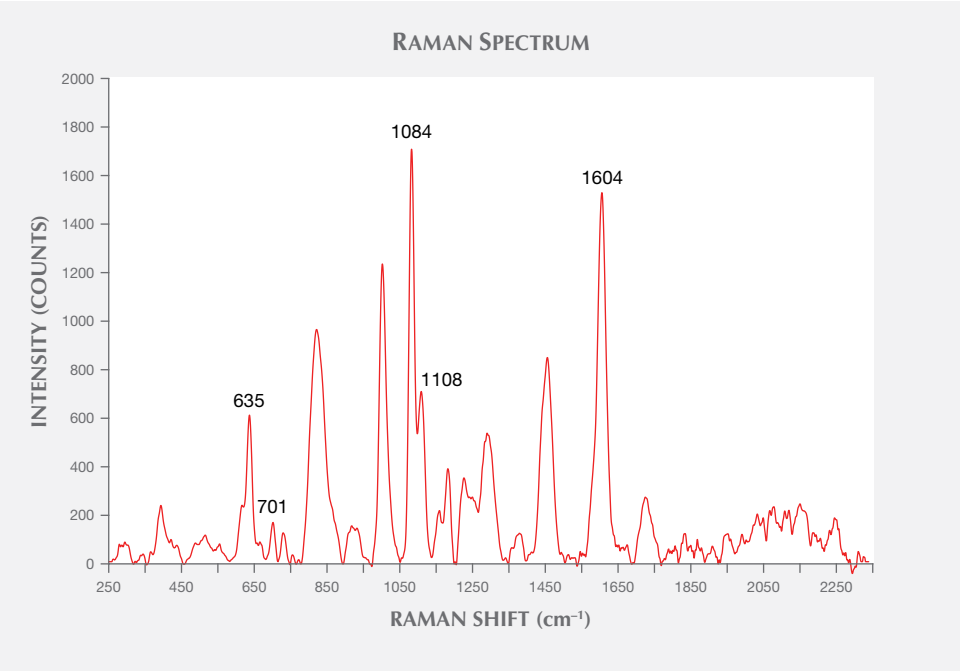

Figure 26. Raman analysis of the pearl revealed epoxy peaks at 635, 1108, and 1604 cm^{-1} and aragonite peaks at 701 and 1084 cm^{-1}.

26). These were consistent with results from FTIR reflectance spectrometry that showed calcium carbonate in the form of aragonite, with peaks at approximately 878 and 1484 cm^{-1}.

X-radiography (figure 27) proved this was a bead-cultured pearl with a pre-drilled nucleus typically used in freshwater pearl cultivation. The filling was very shallow due to the presence of mother-of-pearl (not visible). Energy-dispersive X-ray fluorescence (EDXRF) analysis detected higher levels of manganese, confirming the pearl's freshwater origin. The result came as a surprise to the client, who was expecting confirmation of a natural pearl. Such coatings and fillings, which we have seen before, show the importance of obtaining a reliable laboratory report when purchasing such a large pearl.

Figure 27. X-radiography proved this was a bead-cultured pearl. The filling was very shallow due to the presence of mother-of-pearl (not visible). Image by Lai Tai-An Gem Lab.

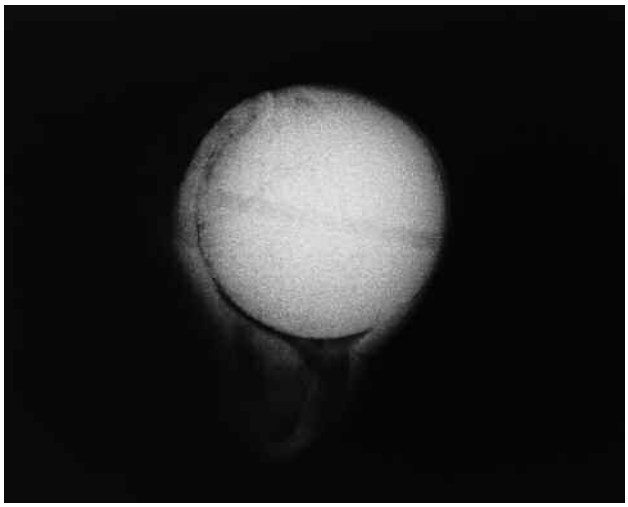

Larry Tai-An Lai (service@laitaian.com.tw)
Lai Tai-An Gem Laboratory, Taipei

Update on dyed hydrophane opal. Dyed purple opals first appeared in the gem trade in 2011 (N. Renfro and S.F. McClure, "Dyed purple hydrophane opal," Winter 2011 *G&G*, pp. 260–270). Recently, the authors became aware of similar material with vibrant blue and pink bodycolors (figure 28). From 2015 to 2017, a jewelry designer reportedly purchased over 500 carats of vivid pink and blue opals from a dealer she met at a small regional gem show in California. The dealer did not disclose that the material was dyed and claimed that these intense colors were from a new opal discovery in Mexico. This kind of misrepresentation could damage consumer confidence in all opals.

In July 2017, author EB received the two opals in figure 28 for examination. After determining that they were likely color treated, he sent both samples to GIA's Carlsbad lab for further testing. With permission from the owner, each opal was cut in half to obtain a control sample and a test sample. The test samples (one blue and one pink) were soaked in acetone and hydrogen peroxide solutions to determine if their colors were stable. These two opals were carefully examined and, like the dyed purple material from 2011, were consistent with hydrophane opal from Ethiopia that had been dyed. Both stones displayed a "digit pattern" play of color (B. Rondeau et al., "On the origin of digit pat-

Figure 28. These two opals (21.75 and 15.12 ct) were represented as natural-color blue and pink opal from Mexico. Photo by Robison McMurtry.

terns in gem opal," Fall 2013 *G&G*, pp. 138–146). They also showed small spots of saturated color at the surface, consistent with dye (figure 29).

Both stones were soaked in acetone to collect some of the dye material for color spectroscopic analysis. The acetone with residual dye was measured and artificially concentrated by a factor of 20 by multiplying the very low absorption values measured. The measurements produced a spectrum consistent with an organic dye, characterized by broad band absorption features in both the pink and blue samples (figure 30). The absorption measurements were then converted to transmission spectra using GRAMS/AI spectroscopy software by Thermo Fisher Scientific. Color space coordinates were calculated from the transmission spectra and plotted as a color swatch. The hues produced were consistent with the bodycolor of each opal, confirming that the spectra represent the organic dye component (figure 30, inset).

The two samples were further tested to see if they could be restored to their original non-dyed state. As reported by Renfro and McClure (2011), soaking dyed purple opal in a solution of hydrogen peroxide removed the purple color. These new pink and blue samples were sliced in half and one piece of each sample was soaked in 3% hydrogen peroxide for up to two weeks. Their color saturation was significantly reduced, with the blue half turning white and the saturated pink half becoming very light pink (figure 31). It is possible that more time in the solution would have further reduced the pink color. Note that even though the samples lost their color, the dye molecules were not removed. But the hydrogen peroxide had oxidatively decomposed the dye into different molecules that did not absorb visible light and therefore could no longer impart color on the opals. Soaking dyed stones in hydrogen peroxide may be an effective way to remove the observed color in dyed opals, returning them to their natural appearance. In our experience, however, there is a risk of cracking when any hydrophane opal is immersed in a liquid.

Acetone allowed the removal of enough dye for spectroscopic analysis, proving that the coloring agent is an organic dye. While soaking the opals in acetone did not seem to greatly affect their color, soaking them in a hydrogen peroxide solution for several weeks removed the artificial color almost entirely. Upon further examination, we determined that they were originally hydrophane opals with a white bodycolor, likely from Ethiopia, that were color treated using an organic dye. These findings reaffirm the

Figure 29. Both the blue and pink opal showed dye color concentrations around pits and scratches on the surface, consistent with hydrophane opal that has been artificially dyed. Photomicrographs by Nathan Renfro; fields of view 2.34 mm (left) and 1.99 mm (right).

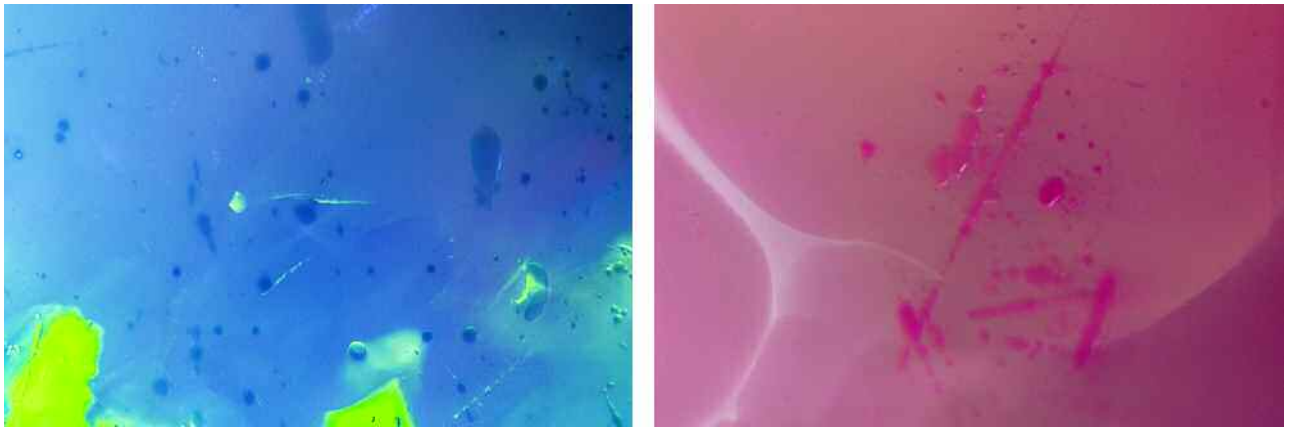

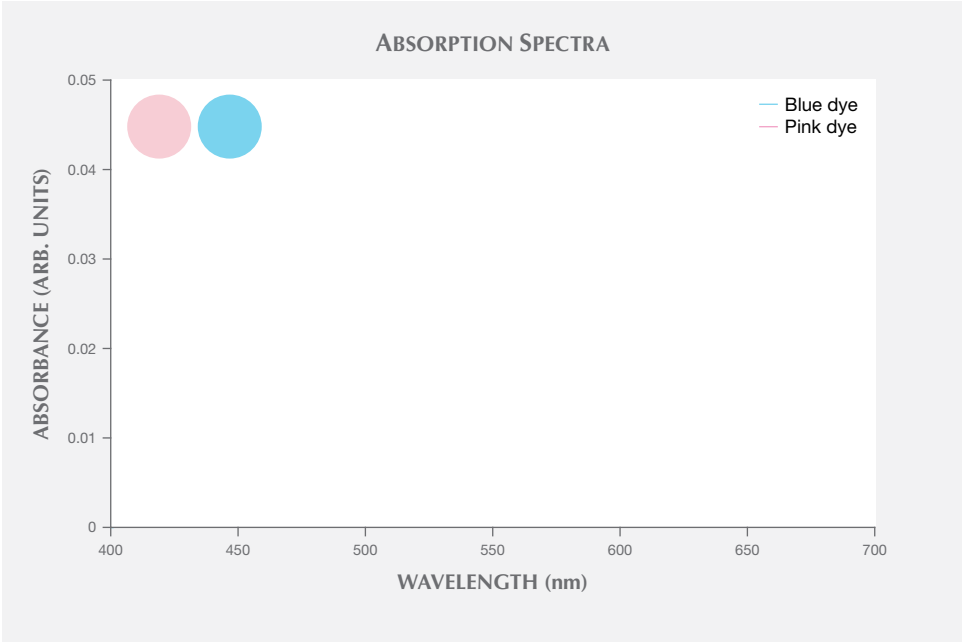

Figure 30. The absorption spectra of the dyes were collected by first soaking the opals in acetone to remove some of the dye material. Color swatches were then calculated from measurements of the dye molecules suspended in acetone to produce the color swatches for reference (inset). These swatches were consistent with the observed bodycolor of each opal.

importance of treatment disclosure in the trade. A few unscrupulous industry members could compromise the reputation of dealers selling natural opal as well as those properly disclosing treated material to their customers.

Edward Boehm
RareSource, Chattanooga, Tennessee
Nathan Renfro
GIA, Carlsbad

Figure 31. The blue and pink opals were confirmed to be dyed hydrophane opal, likely from Ethiopia. Half of each stone has been bleached using 3% hydrogen peroxide solution. Photo by Robison McMurtry.

CONFERENCE REPORTS

GSA 2017 annual meeting. The Geological Society of America (GSA) held its annual meeting October 22–25 in Seattle. For the fifth year, GIA hosted technical sessions on gemological research in the 21st century. More than 30 researchers, students, and gem experts from multiple institutions shared their most recent research results (figure 32).

Invited speaker **Evan Smith** (GIA, New York) presented the diamond inclusion suite study he carried out over the past two years. Following his paper published in *Science* on type IIa Cullinan-like, large, inclusion-poor, pure, irregular, resorbed (CLIPPIR) diamonds, Dr. Smith investigated *in situ* mineral phases in more than 20 extremely rare type IIb diamonds selected from GIA's day-to-day grading operations. The identified inclusions indicated that type IIb diamonds can originate from the lower mantle, at depths beyond 660 km. This surprising result refuted the well-accepted view that almost all superdeep diamonds are small and not of gem quality. **Nancy McMillan** (New Mexico State University) talked about the diamond provenance study she performed with **Catherine McManus** (Materialytics, Killeen, Texas). To ease consumer concerns about conflict diamonds, they conducted multivariate analysis of laser-induced breakdown spectroscopy (LIBS) on diamonds from various origins as well as synthetic diamonds. The information provided by LIBS on trace element composition and the electronic structure of atoms in diamonds aided in provenance determination. Through infrared (IR) mapping, **Sally Eaton-Magaña** (GIA, Carlsbad) and her colleague **Troy Ardon** documented the spatial changes of the optical defect center B^0 (uncompensated boron) in two type IIb diamond samples: One specimen was irradiated along an edge and

Figure 32. Presenters, session advocates, and senior executives from GIA at GSA's annual meeting in Seattle. Photo by Tao Hsu.

then annealed, while the other was only annealed. The irradiated diamond showed an obvious gradient in B^0 across the specimen itself and larger gradient changes during annealing compared to the other sample. These were caused by changes in compensating defects, which were then plotted by photoluminescence (PL) mapping.

The following three presenters from the University of Alberta shared their intriguing diamond formation research. **Mandy Krebs** offered trace element data of fluids trapped in gem-quality diamonds and compared them to those in fibrous diamonds that have been extensively studied. The results showed clear similarities in trace element patterns in both categories, which indicates that fibrous diamonds and gem diamonds may share a common origin. **Rebecca Stone** reported on diamond growth in saline fluid. She and her colleagues carefully documented diamond growth features under different salinities using a mixed KCl-NaCl brine system within the diamond stability field. Their series of experiments showed that Na-rich brine is a better medium for diamond growth than K-rich or Na+K mixed brines. **Robert Luth** discussed the partial melting mechanism facilitating diamond formation. He noted that the amount of diamond formed during this process depends on the lithology being melted and the composition of the fluid. The origin of the C-bearing fluid was also explored.

Following the diamond research presentations, invited speaker **Darrell Henry** (Louisiana State University) started the colored stone session with a talk on gem tourmaline. He pointed out that tourmaline is a very sensitive mineral that can incorporate and retain chemical and textural fingerprints from its environment. Paraíba, Paraíba-like, liddicoatite, and "chrome" tourmaline were used to illustrate this mineral's incredible scientific value. **Aaron Palke** (GIA, Carlsbad) discussed his recent findings on demantoid garnet's coloration mechanism. The existing theory attributes the brown coloration of this gem to intervalence charge transfer between Fe^{2+} and Ti^{4+} or Fe^{3+}. Dr. Palke challenged this interpretation based on recent spectroscopic results showing insufficient Fe^{2+} in demantoid to justify this mechanism. **Philippe Belley** (University of British Columbia) addressed the challenges of modeling spinel deposits. His potential solutions are based on detailed petrographic and geochemical studies on 14 samples from exceptionally well-exposed *in situ* spinel occurrences on Baffin Island in Nunavut, Canada. **Donald Lake** (University of British Columbia) compared two beryl occurrences in northern Canada with Colombian emerald deposits. He pointed out that in terms of formation environment, these potential emerald deposits are the first "Colombian-type" sources outside Colombia. **Rachelle Turnier** (University of Wisconsin–Madison) presented her study on oxygen isotope fractionation factors in corundum. Oxygen isotope ratios are important to understanding corundum genesis and origin determination. This study empirically calibrated the calcite-corundum oxygen isotope fractionation factor from the metamorphosed karst-bauxite deposits at Naxos, Greece. GIA's **Jennifer Stone-Sundberg** closed this portion of the session with a presentation on matrix-matched corundum standards development. She explained the importance of these newly developed standards in accurately determining trace element concentration and elaborated on the advantages of these standards over other commonly used products.

This year's poster session attracted 18 presenters, triple the number from last year (figure 33). **Daniel Howell** (Uni-

versity of Padua) presented new applications of DiaMap software in automated and semi-automated mapping of single substitutional defects (N and B) and micro-inclusion-bearing diamonds. **Paul Johnson** (GIA, New York) reported the first observation of nickel as the cause of the green color of an HPHT synthetic diamond. Nickel is commonly used in the metal flux that produces HPHT synthetic diamond, but it rarely contributes to diamond coloration. **Tyler Sundell** (Missouri State University) evaluated the viability of *in situ* $\delta^{13}C$ measurement in diamonds using time-of-flight secondary ion mass spectrometry (ToF-SIMS). **Tingting Gu** (GIA, New York) shared her study on micro- and nano-inclusions containing both N and Fe in type IaB diamonds. **Kyaw Soe Moe** (GIA, New York) presented the identification features of irradiated and annealed pink diamonds using IR spectroscopy and DiamondView imaging. **Elizabeth Levy** (Louisiana State University) explained how to directly measure Fe^{2+} and Fe^{3+} concentration in tourmaline crystals using synchrotron-based X-ray absorption near-edge spectroscopy (XANES). **Cole Mount** (New Mexico State University) found that using multivariate analysis of LIBS spectra of tourmaline can remove the negative influence of chemical zoning on host lithology determination. **Ulrika D'Haenens-Johansson** (GIA, New York) gave her insights on the 812 ct Constellation and two other large rough diamonds. FTIR and morphology observations indicate that the three could possibly be pieces from the same rough. **Christopher M. Breeding** (GIA, Carlsbad) described the first ever co-occurrence of magnesite, olivine, graphite, and silicon-vacancy defects in natural diamonds and explored the unusual conditions under which these diamonds formed. **Karen Smit** (GIA, New York) discussed the formation of peridotitic diamonds through isochemical cooling and eclogitic diamonds through redox buffering. **George Harlow** (American Museum of Natural History, New York) and **Rachelle Turnier** discovered that syenite-hosted sapphires from six different sources show a wide range of $\delta^{18}O$ values, which indicates scavenging of sapphire from multiple reservoirs. **Troy Ardon** (GIA, Carlsbad) used IR mapping, cathodoluminescence (CL) imaging, and hyperspectral mapping to correlate various optical and infrared point defects in diamonds with strong brown coloration. **Susanne Schmidt** (University of Geneva) outlined U-Pb geochronology work done on zircon inclusions in Sri Lankan sapphires. This study was performed by her former graduate student **Emilie Elmaleh. Ziyin Sun** (GIA, Carlsbad) investigated the role of chromophore vanadium in coloration of pyrope-spessartine garnet, using samples without a color-change phenomenon. **Eric Brinza** (University of Wisconsin–Eau Claire) described an IR spectroscopic study on hydrothermal quartz crystal. Different hydroxyl species concentrations vary both vertically and horizontally through the crystal. **Kyle Tollefson**, also of the University of Wisconsin–Eau Claire, presented IR and visible spectroscopic study on coloration of watermelon tourmaline. The results showed that the chromophore was incorporated during crystal growth and could reflect changes in the growth environment. **Dona Dirlam** and her coauthors from GIA's Richard T. Liddicoat Gemological Library and Information Center (Carlsbad, California) chronicled the legendary John Sinkankas, whose collection of books and other publications was acquired by GIA in 1988 to form the basis of its world-renowned gemological library.

Tao Hsu, James E. Shigley, and Dona Dirlam
GIA, Carlsbad

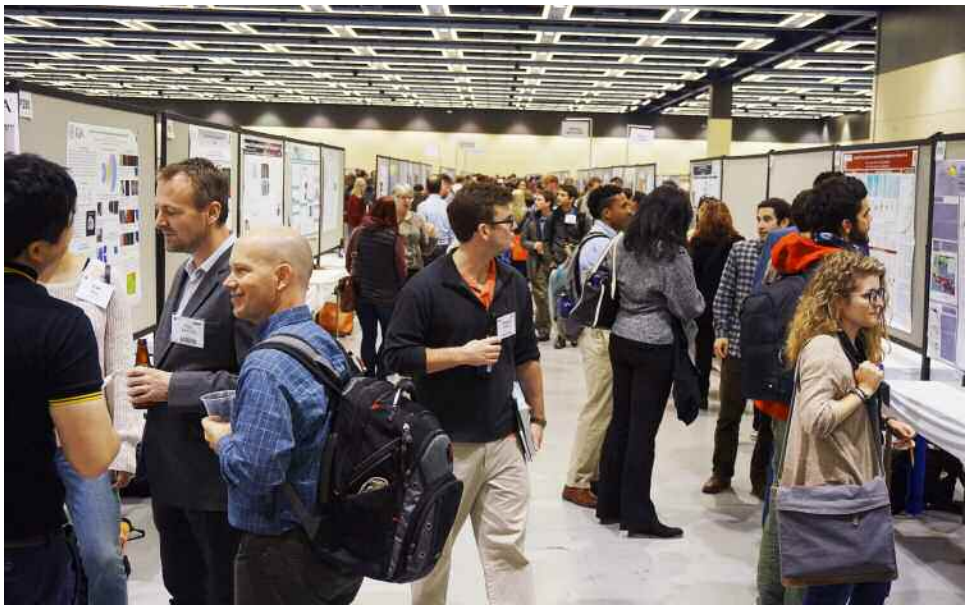

Figure 33. The GSA annual meeting's gemological research poster session featured 18 presenters from all over the world. Photo by Cathy Jonathan.

Figure 34. A gathering of the presenters at the fifth World of Gems Conference, held in Chicago in September 2017. Photo by Scott Drucker.

World of Gems Conference. The Gemworld International team, headed by **Richard Drucker**, hosted the fifth World of Gems Conference September 23–24 at the Loews Hotel in Chicago. The event was bookended by optional classes, making it an ideal opportunity for attendees to learn about new topics from a diverse group of international speakers (figure 34) and brush up on their practical gemology skills. Between presentations, the conference held its first-ever poster session. The posters included interactive discussions on jet and the identification of light blue stones using the polariscope and the conoscope, hosted by **Sarah Caldwell Steele** (Ebor Jetworks, Whitby, United Kingdom) and **Kerry Gregory** (Gemmology Rocks, Weavering, United Kingdom), respectively.

Invited speaker **Emmanuel Fritsch** (University of Nantes, France) opened with a talk about the identification of melee synthetic diamonds. He noted that while the majority of specimens are not hard to identify, near-colorless HPHT-treated synthetic melee may still be challenging. Dr. Fritsch also provided a brief history of synthetic diamond production and the current state of the industry, as well as basic and advanced methods of separating synthetic from natural. Isotropy and anomalous double refraction—otherwise known as strain—were covered in some detail, as he considered these very useful identification aids. **Jon Phillips** (Corona Jewellery Co., Toronto) reviewed world diamond production and the output of mines such as Jwaneng in Botswana, which accounts for 15% of total global production. Meanwhile, Canada's five operating mines rank among the top 19 producers. One key takeaway from his talk was that De Beers plans to invest US$140 million on a marketing campaign aimed at women buying diamond jewelry for themselves. This should not be ignored by jewelers. Mr. Phillips also reflected on the threat of synthetic melee in the market. **This author** (GIA, Bangkok) reviewed the different types of pearls (nacreous and non-nacreous) seen in the market and the various mollusks that produce them. The presentation detailed the surface structures of a wide selection of non-nacreous pearls and concluded with a summary of the more frequently encountered treatments. **Roland Schluessel** (Pillar & Stone International, San Francisco) provided a comprehensive look at Burmese jadeite and defined the various types, including the term *fei cui* (kingfisher) for the vivid green variety. He examined cultural aspects and discussed factors such as grain size and orientation, which relate to transparency and overall quality. Mr. Schluessel also provided insight into the different colors and patterns, as well as the differences between omphacite and jadeite. **Çiğdem Lüle** and **Stuart Robertson** (Gemworld International, Glenview, Illinois) reported on various gem treatments that provide enough supply to satisfy market demand. Frequently encountered treatments and the pricing of untreated vs. treated material were reviewed. Diamond was offered as an example of a gem where treatments markedly affect the end value, while tanzanite shows little if any price difference between natural and treated material. A very lively presentation from **Kerry Gregory** about the daily happenings in the pawnbroking world rounded out day one. Ms. Gregory discussed some of her experiences saving valuable pieces that would have otherwise been destroyed due to lack of resources, training, and time. She also provided insight into her use of simple yet valuable gemological methods (such as the polariscope and conoscope) in identifying light blue stones removed from items destined for the melt.

J.C. (Hanco) Zwaan (Netherlands Gemmological Laboratory, Leiden) started the second day with a comprehensive look at the geological formation and gemological

characteristics of metamorphic sapphires from Sri Lanka and to a lesser extent Montana. The search for a primary sapphire deposit in Sri Lanka and the discovery at Wellawaya (which Dr. Zwaan was involved with) were illustrated. Subsequent discussions on the use of chemical plotting in the separation of Sri Lankan and Montana material, from one another and from other sources, showed that it is beneficial but care is still needed with some cases that may overlap. **Çiğdem Lüle** followed with a solo talk about the various natural and "non-natural" black gem materials and the limitations encountered when testing such materials. She covered black diamonds in some detail, outlining the differences between the rare naturally colored stones and heated or irradiated specimens. **Al Gilbertson** (GIA, Carlsbad) reported on the status of GIA's fancy-cut diamond grading project and showed the challenges faced when producing a system that takes all variables into consideration and satisfies all opinions. This was reinforced after receiving feedback from 440 participants in six global locations who were asked to look at various fancy cuts and answer a series of questions. **Alan Bronstein** (Aurora Gems, New York) took attendees on a journey through the colorful world of fancy-color diamonds, looking at the subtleties of the main colors available: yellow, orange, pink, red, green, and blue. Mr. Bronstein was clearly in favor of retaining the original cut of a diamond and not re-cutting it. Chameleon diamonds were also briefly covered. "Beauty trumps rarity" was Mr. Bronstein's motto. **Richard Drucker** brought the presentations to a close with a look at some challenges that affect the pricing of gemstones. From the small print in pricing guides that might not be fully understood by users to gemological reports that raise doubts or cause confusion in appraisers' minds, it became very apparent that the valuation of some colored stones needed careful thought.

The conference ended with a Q&A session in which Mr. Drucker opened the floor to all attendees. Topics such as correct nomenclature and disclosure, brand name cooperation with items submitted for valuation, and color diamond grading consistency were covered.

Nicholas Sturman
GIA, Bangkok

IN MEMORIAM

Peter J. Dunn (1942–2017). Distinguished mineralogist and author Pete Dunn died November 8 at the age of 74. He is best known for the 134 new mineral descriptions he wrote over the course of his long career.

Dr. Dunn received his master's degree and PhD in mineralogy/geology from the University of Delaware in Newark. Before joining the Smithsonian Institution's National Museum of Natural History in 1972, he served in the U.S. Air Force and worked at Boston University as a curator in the geology department. In addition to characterizing new minerals, Dr. Dunn published a nine-volume monograph and more than 70 papers on the Franklin–Sterling Hill mining district in New Jersey in a number of scientific publications. In 1987, a member of the clinopyroxene subgroup from the Franklin mining district was named "petedunnite" in his honor. A prolific contributor to *G&G* throughout the 1970s, Dr. Dunn served on the journal's editorial review board from its inception in 1981 until 1987. Upon his retirement from the National Museum of Natural History in 2008, he volunteered at the museum's information desk until his death.

ERRATA

1. In the Fall 2017 Lab Note on screening of mounted melee using the GIA iD100 (pp. 366–367), a citation directed readers to p. 239 of the Fall 2017 Lab Notes section. The correct issue is Summer 2017, p. 239.
2. Also in the Fall 2017 Lab Notes section, the inset photo in figure 4 was taken by Kyaw Soe Moe.